Mechanical and structural consequences of associative dynamic cross-linking in acrylic diblock copolymers

*Jacob S. A. Ishibashi,[1] Ian C. Pierce,[1] Alice B. Chang,[2] Aristotelis Zografos,[2] Bassil M. El-Zaatari,[1] Yan Fang,[1] Steven J. Weigand,[3] Frank S. Bates,[2] and Julia A. Kalow[1]**

[1]Department of Chemistry, Northwestern University, Evanston, IL 60208

[2]Department of Chemical Engineering and Materials Science, University of Minnesota, Minneapolis, Minnesota 55455

[3]Argonne National Laboratory, 9700 Cass Ave, Lemont, IL 60439

For Table of Contents use only:

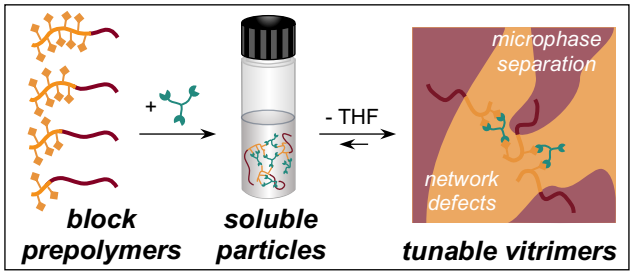

Abstract

The composition of low-T_g *n*-butylacrylate-*block*-(acetoxyaceto)ethyl acrylate block polymers is investigated as a strategy to tune the properties of dynamically cross-linked vinylogous urethane vitrimers. As the proportion of the cross-linkable block is increased, the thermorheological properties, structure, and stress relaxation evolve in ways that cannot be explained by increasing cross-link density alone. Evidence is presented that network connectivity defects such as loops and dangling ends are increased by microphase separation. The thermomechanical and viscoelastic properties of block

copolymer-derived vitrimers arise from the subtle interplay of microphase separation and network defects.

Introduction

Block copolymers that combine rubbery and glassy segments self-assemble into nanostructured materials with emergent properties not seen in the individual homopolymers. These properties are highly tunable by adjusting the volume fraction of each block and their architecture.[1] When the low-T_g segment is the majority block, microphase separation produces a rubbery matrix physically cross-linked by spherical glassy domains. Thermoplastic elastomers (TPEs), the most commercially successful example of this phenomenon, combine the processability of thermoplastics and the elasticity of chemically cross-linked rubbers.[2] As the volume fraction of the glassy block is increased, high-impact thermoplastics with bicontinuous morphologies are formed.[3] Above the T_g of the glassy block, these block copolymers behave as viscous liquids, enabling extrusion and injection molding of virgin and recycled material; however, this transition also defines the upper operating temperature of the material. Under stress, chain pull-out from the hard domains can also occur, ultimately leading to failure. To replace or reinforce these physical cross-links without sacrificing processability, researchers have explored various supramolecular interactions, including H-bonds,[4,5] metal-ligand interactions,[6–8] π-π stacking,[9] and ionic interactions.[10,11]

Here, we explore the incorporation of dynamic covalent bonds in rubbery diblock copolymers, varying their composition to create vitrimers with highly tunable properties. Vitrimers are an emerging class of covalent adaptable networks (CANs)[12,13] that also bridge thermoplastics and thermosetting polymers through associative exchange reactions.[14–18] Unlike TPEs, supramolecular networks, and many dissociative CANs, vitrimers exhibit an Arrhenius viscosity dependence rather than a

discontinuous viscosity drop at elevated temperatures, because reconfiguration of the network topology occurs without loss of covalent connectivity. Furthermore, the associative mechanism is thought to provide higher solvent resistance, since many vitrimers can swell in good solvents without dissolving. Following pioneering work by Bowman and Leibler,[19,20] many researchers have adapted various associative exchange reactions for use in vitrimers. These efforts have focused on controlling vitrimer flow through applying new reactions,[21–26] catalyzing bond exchange,[22] or modifying reactivity of existing mechanisms.[27] Macromolecular structure and assembly might also be harnessed to tune vitrimer properties. For example, cross-link density,[28,29] chain mobility,[30] and phase separation[31] have all been investigated in conjunction with vitrimers.

While the first generation of vitrimers focused on high-T_g thermoset-like materials, our group and others have become interested in the challenge of designing catalyst-free elastomeric vitrimers.[32–38] With high-T_g materials, even if the small-molecule exchange reaction can occur at low temperatures, it will not proceed appreciably within the network until T_g is exceeded.[23] For low-T_g materials, however, the associative exchange reaction must be carefully considered to enable reprocessing at reasonable temperatures but avoid creep under service conditions. Additionally, the identity and structure of the rubbery polymer matrix can influence the mechanism of the exchange reaction[33] and the rate of flow.[39] The majority of elastomeric vitrimers have used telechelic or randomly grafted prepolymers, resulting in vitrimers with a relatively uniform distribution of the exchangeable groups. Segregating the exchangeable groups into one segment of a block copolymer provides new opportunities to tune the properties of the resulting vitrimer while keeping the chemical identity of the components constant. In particular, self-assembly of the vitrimer by microphase separation into cross-link-rich and cross-link-poor domains can be programmed by the structure of the block prepolymer to dramatically influence the vitrimer's thermomechancical properties. We envisioned that

minority blocks bearing exchangeable groups could serve an analogous role to the glassy domains of TPEs, while conferring the superior solvent and temperature resistance common to vitrimers.

During the course of our study,[40] Sumerlin, Epps, and co-workers reported a glassy vitrimer derived from the symmetric block copolymer poly(butyl methacrylate)-*block*-poly(2-(acetoxyaceto)ethyl methacrylate), or BMA-*b*-AAEMA, wherein dynamic cross-linking occurs solely in the AAEMA block[41] using the vinylogous urethane dynamic cross-link developed first by Du Prez and co-workers.[42,43] They attributed differences in the viscoelastic properties, relative to a statistical copolymer-derived vitrimer, to the presence of phase separation. This initial contribution focused on thin-film structure and suggested the potential of block copolymer-derived vitrimers by comparing their high-temperature stress relaxation and creep with those of a statistical copolymer-derived vitrimer.

To build a more complete picture of the design space surrounding block copolymers as vitrimer precursors, we vary the composition of a low-T_g diblock copolymer to study the effect of weight fraction of the cross-linking domain and study a poly(*n*-butylacrylate)-*block*-poly(2-(acetoxyaceto)ethyl acrylate) (PnBA-*b*-PAAEA) system. We provide the full details of vitrimer synthesis, thermomechanical characterization, stress relaxation, and microphase separated structure. Using dynamic light scattering (DLS) and diffusion-ordered NMR spectroscopy (DOSY NMR), we show that under the influence of dynamic cross-linking, block copolymers evolve from hyperbranched polymers to infinite networks. Dynamic mechanical thermal analysis (DMTA) and stress relaxation measurements reveal that rubbery plateau modulus and flow rates do not increase as expected when cross-linker is increased. We employ small-angle x-ray scattering (SAXS) to assess the microstructure of the prepolymers and vitrimers. By studying this series of vitrimers using this broad suite of techniques, we provide experimental comparisons to recent theories describing vitrimer stress

relaxation and elucidate general strategies for tuning vitrimer properties with block copolymer composition.

Results

Synthesis of prepolymers. We synthesized diblock polymers of *n*-butyl acrylate (nBA) and a ketoester-containing acrylate monomer ((2-acetoacetoxy)ethyl acrylate, AAEA)[44] using reversible addition-fragmentation chain-transfer (RAFT) polymerization.[45] Because more common end-group removal protocols[46] were unsuccessful for this system, the trithiocarbonate chain ends were removed by reductive photolysis.[47] We prepared five prepolymers with increasing mole fraction of AAEA, **Block-13**, **Block-24**, **Block-34**, **Block-48**, and **Block-66,** in which the number refers to the weight% functional monomer present in the prepolymer, as determined by ^{1}H NMR (see SI for details). The length of each block was systematically varied to adjust the morphologies and cross-linking densities of the prepolymers and vitrimers, including minority functional blocks (**Block-13**, **Block-24**, **Block-34**), a symmetrical diblock (**Block-48**), and majority functional block (**Block-66**). **Table 1** shows that the M_n of the copolymers fell within a narrow range, from 8 to 11 kg/mol, with low $Đ$ (1.07 to 1.28). We targeted molecular weights well below the entanglement molecular weight of poly(nBA), 29 kg/mol, to avoid mechanical effects arising from backbone entanglement.[48] All of the prepolymers were viscous liquids. Differential scanning calorimetry (DSC) of these diblock copolymers revealed two T_g's below room temperature, consistent with microphase separation between PnBA (T_g –54 °C) and PAAEA-rich domains (T_g –22 °C, **Figure 1**).

Scheme 1. Synthesis of block copolymers used in this study.

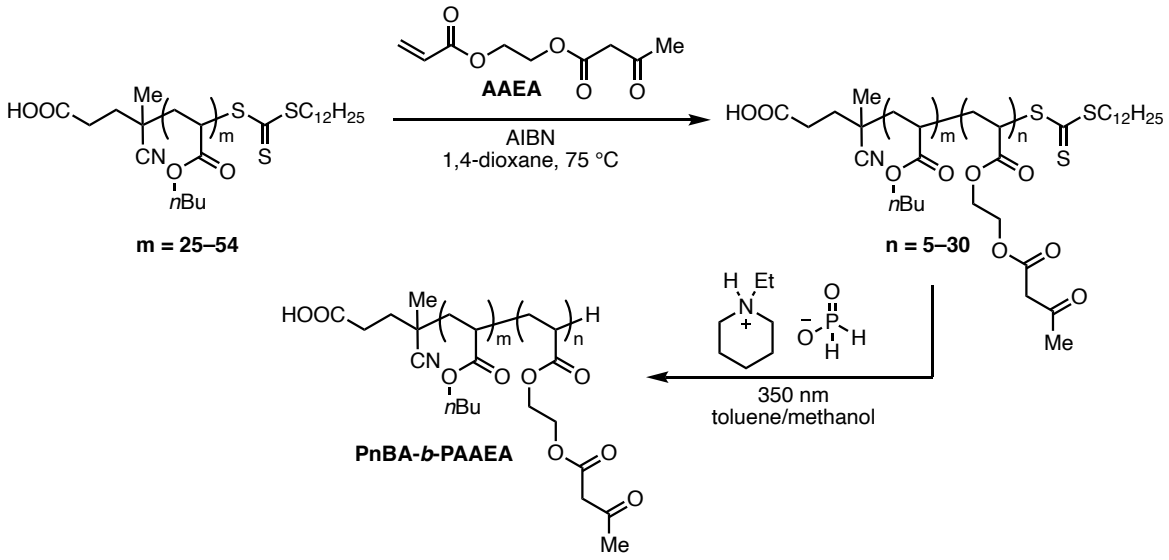

Table 1. Characteristics of PnBA-*b*-PAAEA prepolymers

	Block-13	Block-24	Block-34	Block-48	Block-66
mol% AAEA	9	17	25	37	55
M_n (kg/mol) [a]	8.0	8.3	9.3	11.0	9.2
Đ [a]	1.13	1.18	1.28	1.19	1.07
T_{g1} (°C) [b]	–50	–50	–45	–46	–55
T_{g2} (°C) [b]	–37	–35	–32	–28	–35

[a] Determined by gel permeation chromatography relative to PS standards. [b] Determined by differential scanning calorimetry (second heating cycle).

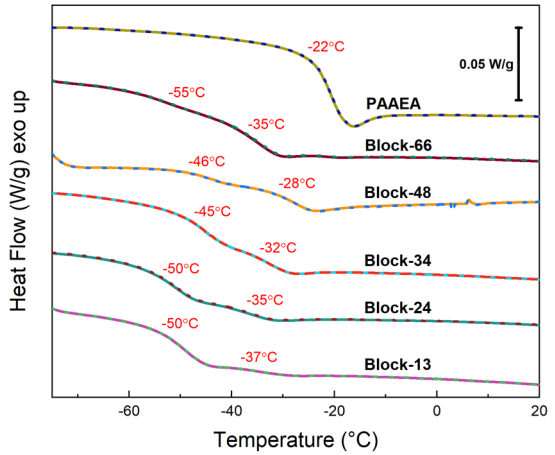

Figure 1: DSC data of all PnBA-*b*-PAAEA prepolymer samples and PAAEA homopolymer with the first heating cycle as a solid line and the second heating cycle as a dotted line (heating rate of 5°C/min).

Cross-linking prepolymers to form vitrimers. To form the vitrimers (denoted with suffix **-Net**), we chose tris(2-aminoethyl)amine (TREN) as the cross-linker, and the theoretical concentration of free primary amine in all networks was 33 mol% excess relative to ketoester functional groups on the polymer (**Scheme 2**). This stoichiometry was previously shown by Sumerlin and coworkers to enable reprocessing on reasonable time scales for poly(methacrylate) vitrimers cross-linked by TREN.[45]

Scheme 2. Cross-linking of the block copolymers by vinylogous urethanes.

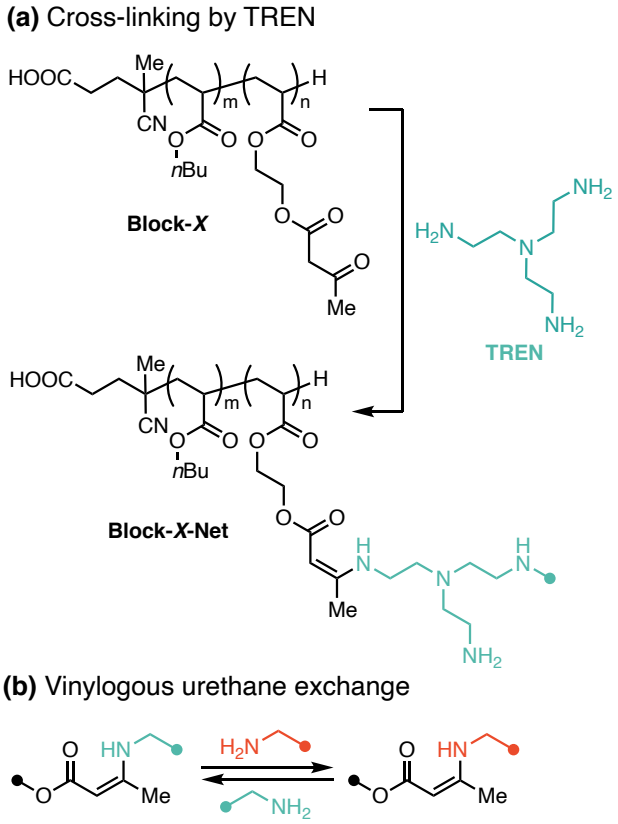

Surprisingly, after adding the cross-linker to the block copolymer solutions (170 mg/mL polymer), we did not observe gelation even after standing in a sealed container overnight. As block-selective covalent cross-linking is a common strategy to stabilize block copolymer micelles,[49] we suspected that

the formation of cross-linked aggregates in solution was occurring instead of network formation. To further understand this phenomenon, we turned to dynamic light scattering (DLS) and diffusion-ordered NMR spectroscopy (DOSY NMR).

DLS of **Block-34** solutions in THF show a peak centered at ~2 nm consistent with unimers and suggesting that the block prepolymers by themselves do not aggregate (**Figure 2a**). Upon adding TREN, cross-linked **Block-34** nanoparticles form quantitatively within minutes. These 10-nm particles do not further aggregate even after 18 hours. These results suggest that ketoester-amine condensation occurs readily, but the prepolymer sequence prevents an infinite network from percolating through the sample at this concentration. Additionally, ^{1}H NMR after addition of TREN in THF-d_8 shows broadening of the signals corresponding to the ethyl linker at 4.3 ppm, and appearance of broad signals at 2.6 and 9 ppm, consistent with successful condensation. The diffusion coefficient of **Block-34** in THF-d_8 is 2.0 x 10^{-6} cm^2/s; after addition of TREN, the diffusion coefficient decreases, indicating the formation of hyperbranched cross-linked polymers with larger hydrodynamic radii. After a week at 25 ºC, gelation is not observed and the diffusion coefficient of the condensed species is 9.6 x 10^{-7} cm^2/s (**Figure 2b**).

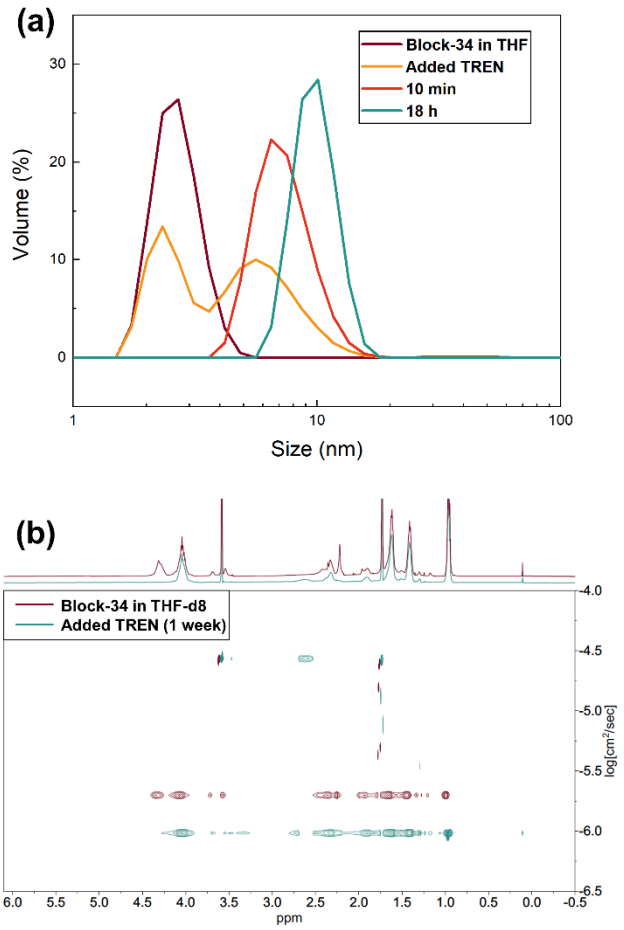

Figure 2. (a) DLS data for solutions of cross-linked **Block-34**. Adding TREN to a 170 mg/mL THF solution of **Block-34** shows that the formation of nanoscale aggregates is relatively fast. Nanoparticles do not change in size after 18 hours. (b) DOSY NMR of **Block-34** in THF-d_8 (10 mg/mL) before and after the addition of TREN.

If a network is to form, the cross-link dynamism must allow for connectivity changes and eventual particle merging, leading toward a critical gel concentration. Indeed, we obtained vitrimers as transparent, pale yellow films after solvent removal and annealing using the following sequence. First, the block copolymer solutions were reacted with TREN, and the solutions were left capped for at least 2 hours to ensure complete conversion of all ketoester moieties.[50] After briefly degassing the solutions using vacuum and a sonicator, we poured the solutions into a mold. The vitrimers were then obtained after slow evaporation of the THF solvent and annealing at 55 °C for 18 hours. A

representative photograph of **Block-66** is shown in **Figure 3**. All the vitrimers in this study had gel fractions (see SI) of 94% or greater (**Table 2**), with the exception of **Block-13**, which remained a tacky, viscoelastic solid at room temperature even after removal of solvent and annealing (**Figures S-17** and **S-18**). The swelling ratios decrease as the amount of functional block increases, as expected based on the increase in sites capable of forming cross-links.

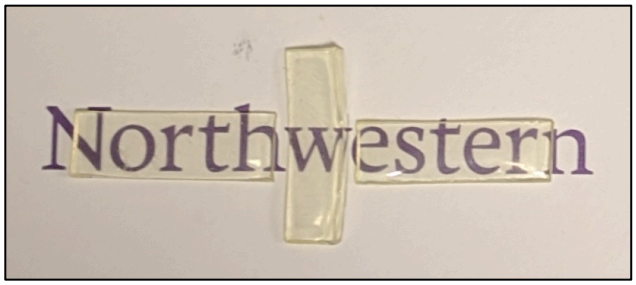

Figure 3. Photograph of **Block-66.** Each sample is approximately 20 x 6.5 x 0.5 mm.

Table 2. Properties of vitrimers

		Block-24-Net	Block-34-Net	Block-48-Net	Block-66-Net
	wt% TREN	7.2	9.9	13.6	17.5
Swelling in THF, 55 °C	**Gel Fraction (%)**[a]	97	94	98	>99
	Swelling Ratio (%)	259	181	128	60
DMTA	$T_{g,1}$ **(°C)** [b]	–31 ± 4	–33 ± 3	-	-
	$T_{g,2}$ **(°C)** [b]	95 ± 1	84 ± 3	106 ± 6	99
	***E'* (MPa)** [c]	2.2 ± 0.1	2.1 ± 0.5	7.0 ± 0.7	30.9
τ* (s)[d]	**190 °C**	49 ± 15	10 ± 4	12 ± 3	11 ± 1
	180 °C	110 ± 55	20 ± 11	18 ± 2	18 ± 3
	170 °C	197 ± 85	40 ± 18	41 ± 9	33 ± 5
	160 °C	408 ± 210	74 ± 36	73 ± 7	62 ± 12
Activation Parameters[e]	E_a **(kJ/mol)**	116 ± 5	112 ± 4	112 ± 16	97 ± 3
	ln(τ_0)	–26.3 ± 1.4	–26.8 ± 1.0	–26.9 ± 4.2	–22.8 ± 0.8

[a] Determination of gel fraction described in SI. [b] Temperature at the peak of tan(δ). [c] Rubbery plateau storage modulus from DMTA at 130 °C. For **Block-24**, **34**, and **48-Net**, the values are the average of three runs. Uncertainty is the Student's T-test. [d] Each value is the average of three runs. Uncertainty is the Student's T-test. [e] Uncertainties are the standard error of the slope and intercept of the Arrhenius plot.

Dynamic Mechanical Thermal Analysis. DMTA of the **Block** vitrimers, which we performed under an atmosphere of nitrogen, reveal a rich viscoelastic landscape (**Figure 4**). **Block-24-Net** and **Block-34-Net** both display a clear drop in their E' traces that is accompanied by a peak in their tan(δ) traces between –28 and –34 °C. This transition corresponds to the T_g of PnBA. As the nBA fraction of the prepolymer decreases in **Block-48** and **Block-66**, the tan(δ) peak corresponding to its T_g disappears. Above –28 °C, E' drops gradually for all samples; this behavior is reminiscent of a thermoplastic and is consistent with the presence of a PnBA domain. This gradual decrease is also similar to DMTA behavior observed by Coates, Hillmyer and co-workers for imine CANs derived from gradient copolymers.[51] In the block copolymer vitrimers, however, the E' and tan(δ) traces display a second, high-temperature transition, corresponding to the T_g of the PAEAA domain. Unlike a thermoplastic elastomer, the E' enters a rubbery plateau instead of terminal flow. The area under this second transition in the tan(δ) trace increases as the volume fraction of the functional block increases. Additionally, the glass transition generally broadens as the cross-linking domain increases in volume.

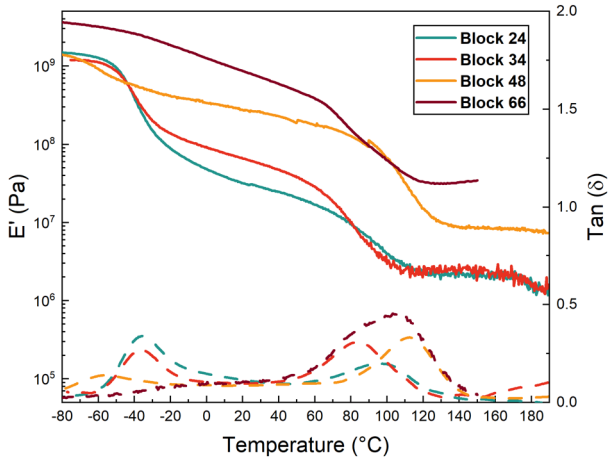

Figure 4. Representative DMTA data: E' (solid lines) and tan(δ) (dashed lines) (heating rate of 3 °C/min).

Curiously, **Block-24-Net** and **Block-34-Net** have statistically similar rubbery plateau moduli E' despite the greater fraction of functional monomers in **Block-34**. A further increase of the functional block in **Block-48-Net** and **Block-66-Net**, however, increases the rubbery plateau modulus as expected. In contrast, the swelling ratios decrease monotonically as the %AAEA is increased, consistent with increasing cross-link density. These data suggest that the cross-link densities of the vitrimers are different in the dry and swollen states and will be examined further in the Discussion.

Stress Relaxation. CAN recyclability is attributed to the presence of dynamic bonds, which facilitate the rearrangement of network topology to bridge the surfaces of smaller fragments and macroscopically re-form a continuous material. Stress relaxation in vitrimers is considered a fingerprint for recyclability and offers quantitative insight into the timescale required for bond swapping and subsequent topology rearrangement. We performed stress relaxation experiments under an atmosphere of nitrogen at temperatures ranging from 160–190 °C. We chose this range to avoid any complexities related to the glass transition. The inhomogeneous structure of the **Block** vitrimers suggests that they would display multiple stress relaxation modes, deviating from ideal Maxwellian behavior. In the context of vitrimers, Torkelson[52] and others have estimated that a stretched exponential (eq 1) can capture these deviations:

$$\frac{E}{E_0} = \exp\left(-\left(\frac{t}{\tau^*}\right)^{\beta}\right) \qquad \text{(eq 1)}$$

E/E_0 is the normalized relaxation modulus, t is the time in seconds, τ^* is the characteristic relaxation time, and β is a fitting factor that is a proxy for the homogeneity of the relaxation process. In the upper limiting case ($\beta = 1$), the relaxation is that of a single Maxwell element (i.e., the material possesses a single relaxation mode), while the lower limiting case ($\beta \sim 0$) represents multiple relaxation

modes. In the case of the block-copolymer-derived vitrimers, β values lie between 0.41 and 0.62, suggesting that the materials are indeed inhomogeneous and cannot be accurately represented by a single Maxwell element.

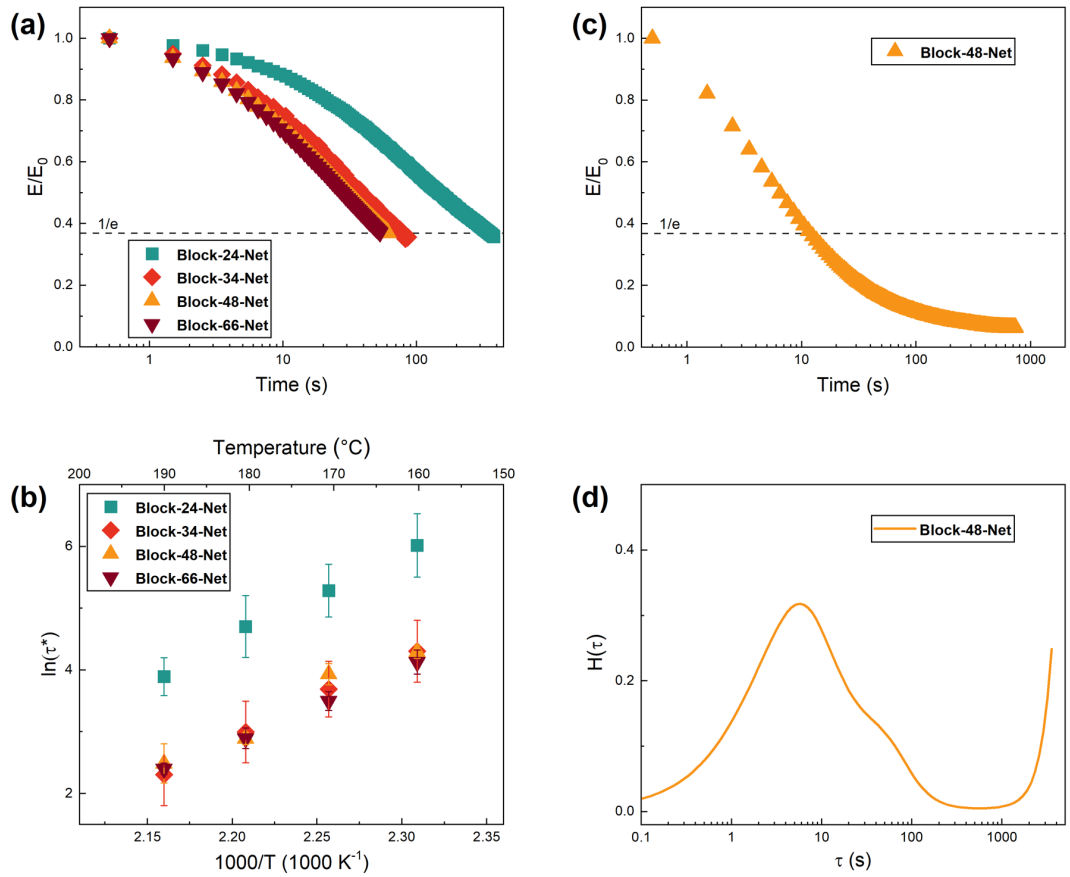

Figure 5. (a) Representative stress relaxation data at 160 °C. (b) Arrhenius plots for stress relaxation in the range of 160–190 °C. (c) Full stress relaxation profile for Block-48-Net at 190°C. (d) Continuous relaxation spectrum for (c).

Flow activation energy E_a may be estimated by fitting τ* data to an Arrhenius-like equation (ESI, Eq S-2). Interestingly, we do not observe a trend in τ* or E_a as the nominal cross-link density (i.e. AEAA fraction) is increased. The vitrimer with the lowest AEAA fraction, **Block-24-Net**, exhibits significantly longer relaxation times. The relaxation times for **Block-34-Net**, **Block-48-Net**, and **Block-66-Net**, in contrast, are nearly identical at 160 °C (**Figure 5a**). In contrast, the E_a values of

Block-24-Net, **Block-34-Net**, **Block-48-Net** are in fact quite similar (112–116 kJ/mol, within error), while that of **Block-66-Net** is slightly lower (97 kJ/mol) (**Figure 5b**, **Table 2**).

A "full" relaxation profile of a **Block** vitrimer shows that a limited amount of stress is retained at long time scales, even at 190 °C (**Figure 5c**). To further support the notion of inhomogeneity in the relaxation process, we obtained the continuous relaxation spectrum of **Block-48-Net** at 190 °C (**Figure 5d**; see SI for details). We found that multiple relaxation modes emerged, including one at extremely long timescale. These data are consistent with creep measurements performed by Sumerlin, Epps, and co-workers, who demonstrated that a symmetrical block copolymer-derived vitrimer was able to resist creep at high temperature, relative to a statistical copolymer-derived vitrimer with identical composition.[41] This resistance to creep was ascribed to restricted strand diffusion in a microphase-separated network structure.

An alternative explanation for the stress retained at long timescales is the formation of permanent cross-links. PnBA is known to undergo amidation by primary amines in the presence of Lewis base catalysts.[53] While our vitrimers lack a catalyst, we do observe trace amide formation when neat PnBA and TREN are heated to 160 ºC for 24 hours (**Figure S-29**). However, we would expect amide formation to affect both block and statistical copolymers similarly, and a control vitrimer derived from a statistical copolymer displays a single relaxation mode and relaxes all stress within 200 s at 190 ºC (**Figure S-23**).

Torkelson has shown that vitrimers can be reprocessed even if they retain some stress at infinite time, provided a permanent network is not fully percolated throughout the material.[52] Indeed, we can reprocess **Block-48-Net** at 120 ºC (2 hours, 10 ram tons), with full recovery of the rubbery plateau modulus and stress relaxation behavior (**Figure S-31**), suggesting that phase separation and/or a small fraction of permanent amide bonds do not hinder reprocessability.

Small-Angle X-ray Scattering. SAXS data confirm microphase separation in **Block** prepolymers and their resulting vitrimers (**Figure 6**). **Block-24** and **Block-34** have SAXS patterns consistent with hexagonally-packed cylinders with principal domain spacing $d = (2\pi/q^*) = 11.9$ nm and 11.3 nm, respectively, where q^* is the first scattering peak, while **Block-48** and **Block-66** have SAXS patterns consistent with lamellae with principal domain spacing 14.3 and 11.1 nm (**Table 3**). **Block-13**, which did not form a network upon addition of TREN, displays a single broad peak by SAXS despite exhibiting two T_g's by DSC. Variable-temperature SAXS data reveal that the order-disorder transition temperature (T_{ODT}) follows the trend **Block-13** << **Block-24** < **Block-34** ~ **Block-66** << **Block-48** (**Figure S-26**). The diblock **Block-48** did not exhibit an ODT up to 215 °C, consistent with its symmetrical structure and slightly higher molecular weight.

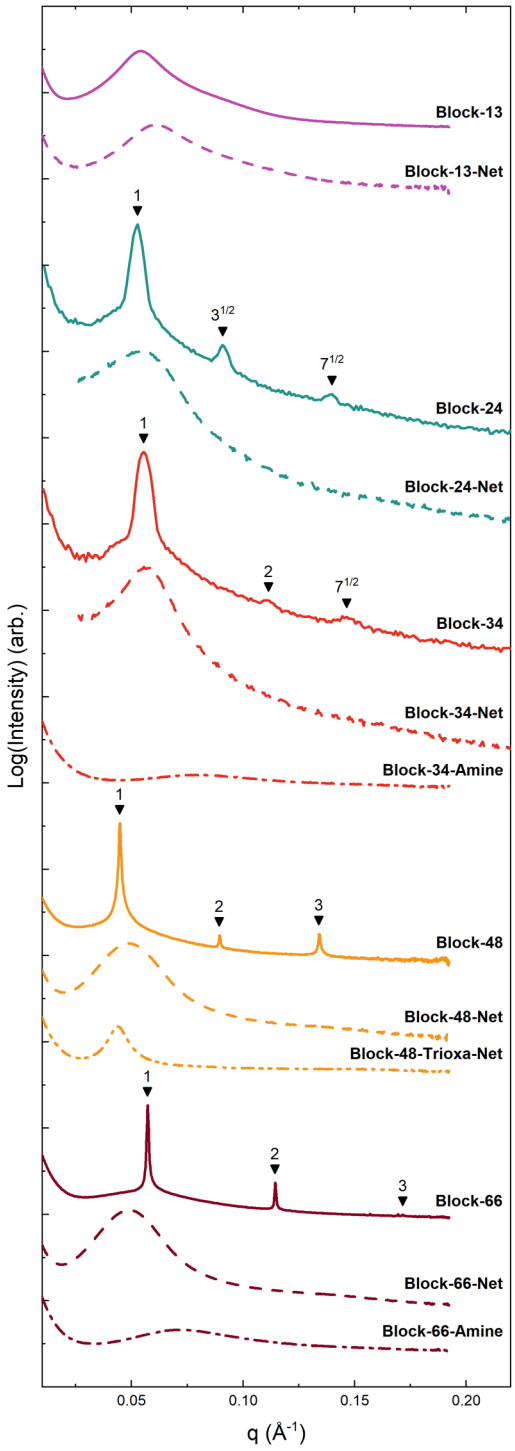

Figure 6. SAXS data for **Block** prepolymers and vitrimers. Curves have been shifted vertically for clarity. Data for **Block-24** and **Block-34** and the corresponding vitrimers were acquired on a lab-based (Ganesha) instrument, while other data were acquired using synchrotron radiation; see SI for details.

Table 3. Morphological characteristics of block prepolymers and vitrimers

		Block-13 [a]	Block-24	Block-34	Block-48	Block-66
Before cross-linking	**morphology**	DIS	HEX	HEX	LAM	LAM
	T_{ODT} (°C) [b]	-	115	135	>215	145
	d (nm) [c]	11.6	11.9	11.3	14.1	11.0
After cross-linking	d (nm) [c]	10.3	11.5	11.1	12.9	12.9
	Δd (%) [d]	–11.6	–3.4	–1.8	–8.1	17

[a] This sample did not form an elastomeric network upon addition of TREN. [b] Lower-bound estimate determined by SAXS from the transition in 1/intensity vs. 1/T (see **Figure S-27**). [c] Determined by SAXS from the first scattering peak, $d = (2\pi/q^*)$. [d] Change in d value before and after cross-linking with TREN.

All vitrimers, in contrast, exhibit a single broad peak by SAXS, suggesting disorganized but microphase-separated morphologies (**Figure 6**, dashed lines). Annealing at higher temperatures or for longer times did not improve the organization of the vitrimers (**Figure S-25**). This disorganization is consistent with what Sumerlin, Epps, and co-workers observed in bulk films obtained by solution-casting their block copolymer-derived vitrimer. All of the samples with PAEAA as the minority or symmetrical block, **Block-13** through **Block-48**, displayed a decrease in the d value after cross-linking, while **Block-66** displayed an increased principal domain spacing after cross-linking.

Clearly, introduction of TREN disrupts long-range ordering of the block copolymer microdomains. We hypothesized that this loss of order could arise from thermodynamic origins if the segregation strength of PnBA-*b*-PAEAA is lowered by formation of the vinylogous urethanes, or by the dramatic increase in dispersity that accompanies branching as cross-links form.[54] Alternatively, disorganization could be ascribed to kinetics if associative cross-linking in the disordered solution state creates barriers to formation of the ordered morphologies. To probe these possibilities, we condensed *N,N*-dimethylethylenediamine onto the representative prepolymers **Block-34** and **Block-66** (**Scheme 3**). This condensation with a primary amine simulates the chemistry of the functional block after cross-

linking but denies the polymers the ability to form a network. In the resulting linear diblock copolymers, **Block-34-Amine** and **Block-66-Amine**, we also observed the loss of order by SAXS (**Figure 6**). These results suggest that the change in chemistry from ketoester to vinylogous urethane side chains reduces the magnitude of the Flory–Huggins interaction parameter, χ, with the PnBA blocks. Attractive interactions between the carboxylate end group (derived from the RAFT chain-transfer agent) and the TREN amines may also compatibilize the blocks.

Scheme 3. Condensation to form linear vinylogous urethane diblock copolymers.

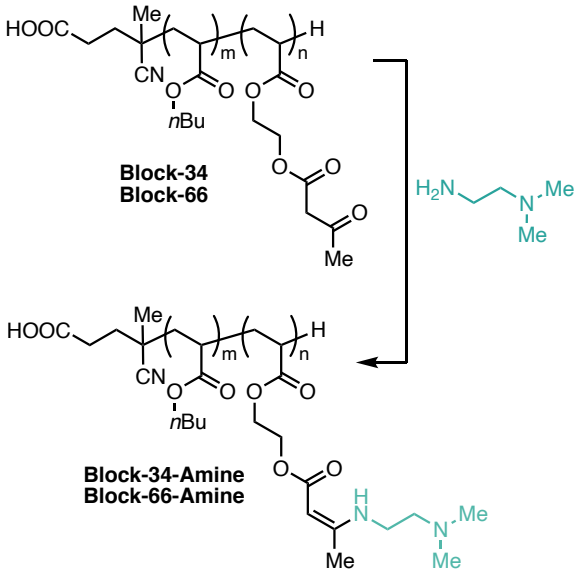

To increase the segregation strength of the cross-linked block copolymer, we next crosslinked **Block-48**, the prepolymer with the highest T_{ODT}, with a polar diamine, 4,7,10-trioxa-1,13-tridecanediamine. We rationalized that this polar linker might disfavor mixing of the crosslinked PAAEA block with the nonpolar PnBA block, and serve as a competitive H-bond acceptor to disrupt any favorable interactions between the vinylogous urethanes and PnBA esters. The resulting annealed vitrimer (**Block-48-Trioxa-Net)** was cloudy, suggesting macrophase separation (**Figure S-16**). Nonetheless, the SAXS pattern in **Figure 6** again exhibited a single peak, which was narrower than that of **Block-48-Net** but still devoid of higher-order scattering peaks, consistent with a disorganized

morphology. Therefore, simply increasing the polarity of the cross-linker is insufficient to drive organization in block copolymer vitrimers.

Dissolving a vitrimer. The vitrimers were formed by removing solvent from a solution of cross-linked nanoparticles, an example of architectural transformation from a hyperbranched polymer to an infinite network.[55] The persistence of the block prepolymer-derived nanoparticles in solution at room temperature suggests that they are thermodynamically stable under these conditions. In principle, therefore, it should be possible to perform the reverse architectural transformation, from an infinite network to soluble hyperbranched polymers, simply by diluting the vitrimer. Recently, Nicolaÿ,[56] Avérous,[29] and Smulders[57] have shown that boronic ester- and imine-based vitrimers can be readily dissolved under mild conditions. While these chemistries are susceptible to hydrolysis from adventitious water, Avérous and Smulders obtained ^{1}H NMR spectra of the dissolved vitrimers showing that imines were retained. These observations are in stark contrast to the prevailing wisdom that vitrimers cannot be dissolved because of the associative exchange mechanism.

As our gel fraction data (**Table 2**, 94–99%) demonstrate, the block copolymer-derived vinylogous urethane vitrimers remain largely intact in THF at 55 ºC, suggesting that there are kinetic barriers to dissolution. Therefore, we conducted experiments at higher temperature, with rigorous exclusion of oxygen and moisture to minimize side reactions that could introduce permanent cross-links[58,59] or hydrolyze the network. Indeed, we observed that **Block-24-Net** swelled and fragmented in THF when heated in a sealed vessel to 110 °C over the course of 48 hours (**Figure 7a,b**). DLS confirms the presence of nanoscale particles in the sol, analogous to the hyperbranched polymers obtained during solution cross-linking (**Figure 7c**). Nevertheless, we did not observe quantitative degradation of the vitrimer even under these forcing conditions, consistent with the associative cross-links enabling local bond rearrangement but resisting macroscopic remodeling. Additionally, slight coloration of the

material suggests trace amine oxidation occurred under these forcing conditions despite our precautions.

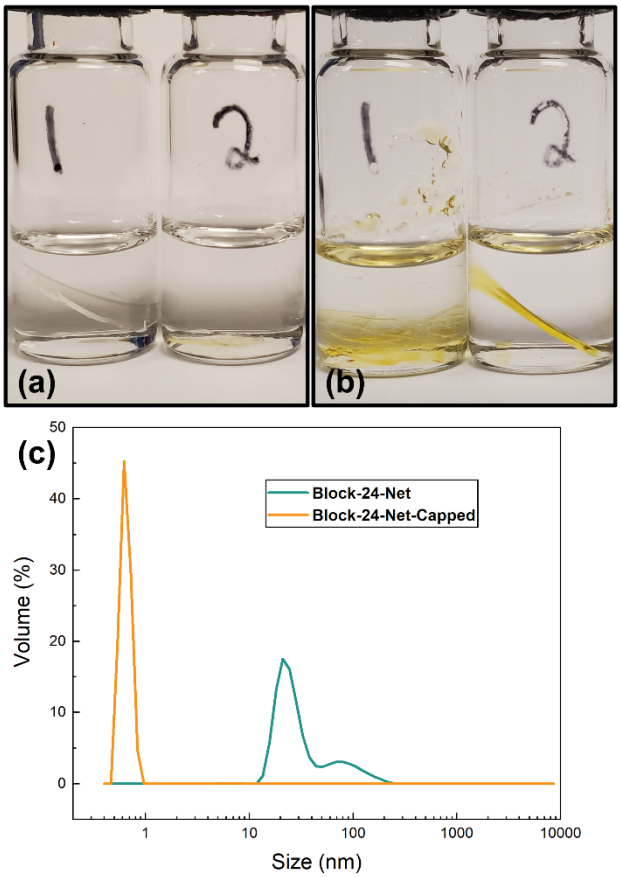

Figure 7. (a,b) Photographs of **Block-24-Net** (labeled 1) and the same material "capped" with methyl acetoacetate (labeled 2) to prevent reconfiguration, before (a) and after (b) heating in THF at 110 °C in sealed vessels. (c) DLS of the sol fractions recovered from the vials in (b).

To confirm that associative dynamic bond rearrangement to form higher-order loops was responsible for partial dissolution of the vitrimer rather than undesired hydrolysis or bond-breaking, we swelled **Block-24-Net** with methyl ketoacetate to consume the excess primary amines (**Block-24-Net-Capped**). Leibler has shown that this small-molecule reaction prevents further rearrangement of the vinylogous urethanes, "freezing" the vitrimer topology.[34] Indeed, the capped vitrimer remained

intact after heating in THF at 110 ºC for 4 days (**Figure 7b**), and no polymer or particles were observed in the sol by DLS (**Figure 7c**).

As is typical for vitrimers, it is possible to quantitatively dissolve the networks in the presence of excess monofunctional amine, which displaces the TREN cross-linker to re-form linear polymer strands. This experiment was performed with **Block-48-Net** and *N*,*N*-dimethylethylenediamine, and GPC traces of the dissolved vitrimer are consistent with **Block-48-Amine** formed from the prepolymer and monofunctional amine (**Figure S-28**), suggesting that the polymer backbone is not modified.

Discussion

The properties of block copolymer-derived vitrimers arise from the subtle interplay of phase separation and network defects. Below, we discuss how these interrelated features influence the formation, thermomechanical properties, and structure of vitrimers derived from phase-segregating block copolymers.

Gelation: the formation of hyperbranched polymers in solution reflects loop defects. The importance of network defects in these materials is most obvious when the block copolymers are cross-linked in solution to form stable 10-nm particles. Even at a relatively high concentration (170 mg/mL) in THF, a good solvent for both blocks, intra-strand cross-linking (i.e., primary loops) and cross-linking among a limited number of block polymer unimers are favored over long-range elastically-effective linkages. The resulting soluble hyperbranched polymers can only exist if a significant fraction of the cross-links is engaged in loop defects. In permanent networks, loop defects increase as the concentration of network precursors decreases, consistent with an intramolecular cross-linking process.[60]

Based on the DLS and DOSY NMR studies, we propose that in solution the block copolymers react rapidly with TREN, consuming ketoester bonding sites and forming hyperbranched polymers rich in primary and higher-order loops. As solvent is removed, bond rearrangement continues to occur until a sufficient number of elastically effective cross-links are forged. A schematic for the proposed process is shown in **Figure 8**. Flory-Stockmayer and Carothers equations, which do not account for network defects, predict that **Block-13-Net** (average functionality of 5.6) should be well over the critical gel point at full conversion of the ketoesters. Nevertheless, **Block-13-Net** did not form the expected elastomeric vitrimer even after removal of solvent.

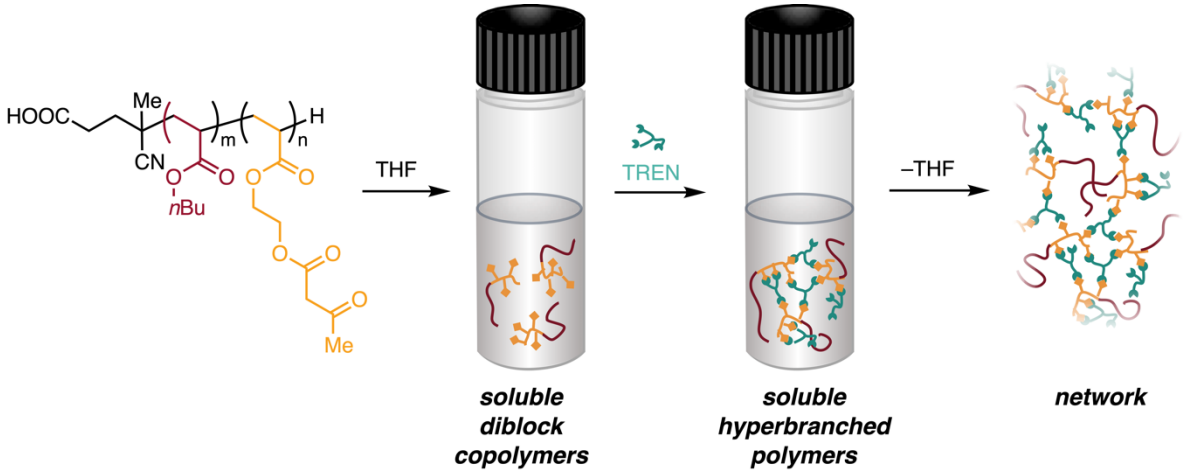

Figure 8. Schematic of the proposed formation of cross-linked hyperbranched polymers and topological transformation to networks upon removal of solvent.

We hypothesize these loop defects are more favorable when the functional monomers are closely spaced, as is the case in the PnBA-*b*-PAEAA prepolymers. Consistent with this hypothesis, statistical poly(nBA-*co*-AEAA) copolymers with 18 or 28 wt% AEAA (**Stat-18** and **Stat-28**) gel rapidly when TREN is added to 170 mg/mL THF solutions, based on the flow inversion test and oscillatory shear rheology measurements (see SI, **Figure S-19**).

This work demonstrates that sequence can affect the connectivity of dynamically cross-linked polymers in solution. This insight can also be useful for processing: block copolymer vitrimers display critical gel points that are a function of concentration, rather than conversion of reactive sites. The solutions of hyperbranched polymers can be exploited in situations where low viscosity is required, then solvent can be removed to form the vitrimer without any additional reagents or stimuli. While associative exchange reactions have been used to transform the architecture of dynamic covalent polymers between linear, lightly cross-linked, and network states, these transformations relied on the addition of competitive nucleophiles.[61] The sensitivity of this vinylogous urethane block copolymer vitrimer system to concentration at ambient temperature more closely resembles supramolecular polymers than typical dynamic covalent systems, which require heat, light, or reagents to trigger reconfiguration.[55]

Thermomechanical properties and swelling ratios: the dry vitrimers have more network defects than the swollen networks. The two T_g transitions of **Block-24-Net** and **Block-34-Net** clearly reflect microphase separation. The lower T_g (–31 to –34 °C) is assigned to the PnBA-rich domain and the higher T_g (84–95 °C) is assigned to the cross-linked PAEAA-rich domain. In **Block-48-Net** and **Block-66-Net**, solely the high-temperature transition is clearly evident by DMTA. The increase in T_g for the PAEAA-rich domain of the vitrimers compared to the prepolymers is expected because cross-links restrict segmental mobility.[62–64] However, the T_g's corresponding to *both* the PnBA- and PAEAA-rich domains increase after cross-linking, suggesting that significant mixing of the blocks has occurred, positioning vinylogous urethane cross-links in the PnBA-rich domains.[65]

Cross-link densities $\upsilon_{modulus}$ for the dry vitrimers can be calculated from the rubbery plateau modulus, E', at 130 °C using eq 2:

$$\upsilon_{\text{modulus}} = \frac{E'}{3RT} \qquad \text{(eq 2)}$$

We observe a non-monotonic trend in cross-link density with increasing % AEAA (**Figure 9**). Specifically, **Block-34-Net** exhibits an anomalously low cross-link density, with similar effective cross-links per unit volume as **Block-24-Net**, despite having approximately 50% higher functionality in prepolymers with similar molecular weight and dispersity. The low crosslink density in dry **Block-34-Net** is also supported by its second T_g (84 °C), which is lower than that of the other vitrimers (95–106 °C).

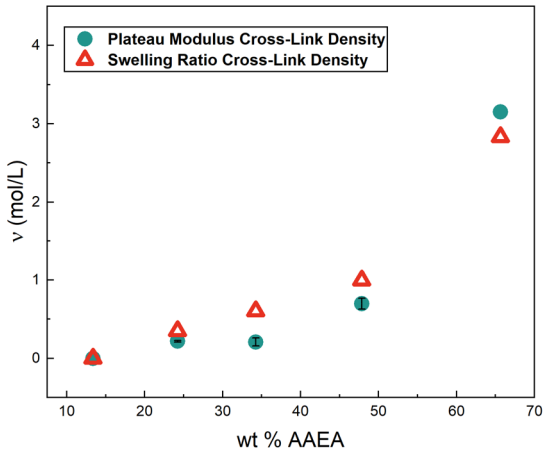

Figure 9. Comparisons of cross-link density calculated for the dry network, calculated from the rubbery plateau modulus using the equation $\upsilon = E'/3RT$ (teal), and the cross-link density calculated for the network swollen in THF, calculated from the swelling ratio using the Flory–Rehner equation (orange).

For permanently cross-linked networks, the cross-link densities calculated from rubbery plateau moduli correspond, albeit imperfectly, to those calculated from swelling ratios because the network topology is the same in the dry and swollen states.[66] In vitrimers, however, if associative cross-link exchange occurs under the conditions of swelling, the swollen networks can adopt different topologies

in the dry and swollen states. The cross-link densities of equilibrated swollen networks, $\upsilon_{\text{swelling}}$, can be calculated using the Flory–Rehner equation (eq 3):[67]

$$\upsilon_{\text{swelling}} = -\frac{\ln(1-v_2)+v_2+\chi_{12}{v_2}^2}{V_1({v_2}^{1/3}-2v_2/f)} \quad \text{(eq 3)}$$

where v_2 is the volume fraction of polymer network in the swollen sample at equilibrium calculated from the swelling ratio, V_1 is the molar volume of THF, f is the average functionality of the prepolymer and TREN, and χ_{12} is the Flory-Huggins polymer-solvent interaction parameter, which we approximate using the literature value for PnBA in THF[68] (see SI for details; χ values for PAAEA and PAAEA condensed with TREN are not known).

Diluting a vitrimer by swelling is expected to decrease the cross-link density relative to a dry network because dilution favors intramolecular crosslinks.[60] Indeed, this trend is observed for other vitrimer chemistries[69] and for our statistical copolymer control vitrimers, **Stat-18-Net** and **Stat-28-Net** (**Table S-8**). It is therefore surprising that the calculated cross-link densities for swollen **Block-24-Net**, **Block-34-Net**, and **Block-48-Net** are *higher* than cross-link densities for the same materials in their dry form (**Figure 9**). Additionally, **Block-34-Net** does not display anomalously low cross-link density once swollen. Even considering the errors in Flory–Rehner theory and the approximations we have made, the discrepancies between $\upsilon_{\text{modulus}}$ and $\upsilon_{\text{swelling}}$ in both their absolute values and their trends suggest that the network topologies of block copolymer vitrimers are altered in the swollen and dry states. While this discrepancy could arise from the loss of low-functionality strands to the sol fraction, which was previously observed in phase-separated polyethylene/dioxaborolane vitrimers with gel fractions <40%,[70] the block copolymer vitrimers described here have gel fractions ≥94%.

The persistence of cross-linked hyperbranched polymers in solution shows that the block copolymer architecture encourages the formation of network defects in solution; we expect that this trend extends

to the network. While directly comparable **Stat** and **Block** vitrimers have not been synthesized, **Stat-18-Net** and **Stat-28-Net** have similar or higher rubbery plateau moduli (1.9 and 4.8 MPa, respectively) than **Block-34-Net** (2.1 MPa), despite having fewer AAEA groups in the prepolymers (**Figure S-21**). Both TREN and the prepolymers have functionality ≥3, but TREN molecules having 1 or 2 free amines can form primary loops and dangling ends, respectively, since these vitrimers are prepared with 33% excess amine. A schematic depicting relevant types of network defects is shown in **Figure 10**. Interestingly, in the case of poly(methacrylate) vinylogous urethane vitrimers, Epps and Sumerlin did not observe a significant difference in the rubbery plateau moduli for vitrimers derived from statistical and diblock copolymers.[41] The prepolymers in that study featured equimolar incorporation of non-functional (nBMA) and functional (AAEMA) monomers, corresponding most closely to **Block-66-Net**. Despite the many similarities of that system to the present one, our use of more flexible acrylic backbones and TREN cross-linker may encourage the formation of loops. Furthermore, the low M_n values of our prepolymers rule out entanglements as contributors to the rubbery plateau moduli. In a clear demonstration of sequence effects on network topology, Alabi prepared homogeneous, permanently cross-linked thermosets from sequence-defined oligomers.[71] A blocky AAAmmm sequence (where A is the cross-linkable unit) yielded significantly lower rubbery plateau moduli than an alternating mAmAmA sequence. This difference was ascribed to the combined effects of dangling chain ends and primary loops.

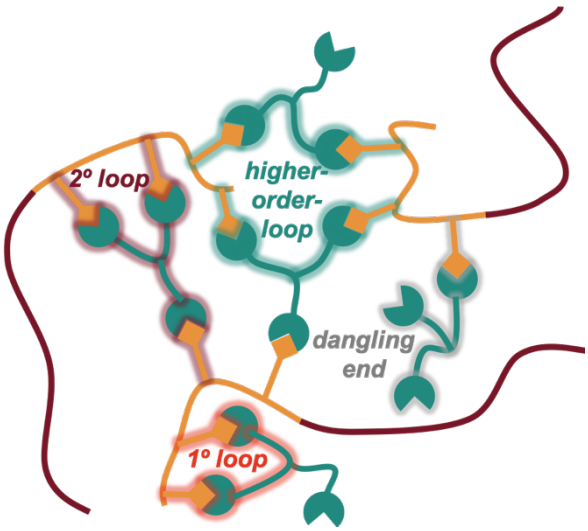

Figure 10. Depiction of different types of network defects that can occur in the block copolymer vitrimers.

Based on evidence of microphase separation from the T_g and SAXS data, we propose that the dry vitrimers have more loop defects than their swollen counterparts because the dry state is microphase separated. This separation creates cross-link-rich PAAEA domains and cross-link-poor PnBA domains. A sufficiently high χ parameter between the blocks could potentially prevent network formation by confining all cross-links to isolated minority domains. In order to percolate an infinite network, "tie strands" of cross-linked PAAEA blocks must mix with the PnBA-rich phase to link cross-link-rich domains. The increase in the T_g of the PnBA phase observed for **Block-24-Net** and **Block-34-Net** is consistent with this scenario. Furthermore, the cross-link-rich phase can achieve an infinite network within a bicontinuous morphology; this scenario is more likely for **Block-48-Net** and **Block-66-Net**, which have higher fractions of the cross-linked block. Unfortunately, SAXS of the vitrimers does not provide insight into the morphology, and TEM imaging was not possible.

Phase separation: dynamic covalent cross-links hinder organization. The domain spacing of the block copolymers before and after associative cross-linking is consistent with loop-rich domains in the vitrimers. For **Block-13** through **Block-48**, the domain spacing shrinks by 1.8–11.6% after

cross-linking. Isono and Satoh have shown that intramolecularly cross-linking one block of a diblock copolymer under dilute conditions significantly reduces the chain dimensions, providing significantly (9–22%) downsized features after bulk self-assembly relative to the non-cross-linked copolymers.[72] In that case, the topology of the polymers can be considered entirely primary loops and no elastically effective cross-links; indeed, in our study, **Block-13-Net** has the fewest elastically effective crosslinks and the largest reduction in domain spacing. In contrast, **Block-66-Net** displays an increase in domain spacing after cross-linking, suggesting the presence of fewer network defects and, possibly, the influence of added TREN, which comprises 17.5 wt% of the vitrimer.

As described in the previous section, the thermomechanical data provides some evidence for phase separation, particularly for **Block-24** and **Block-34**, which clearly possess two T_g's. In contrast to the prepolymers, which form well-defined morphologies depending on their composition, the vitrimers display a single broad scattering peak by SAXS. This disorganization can arise from thermodynamic origins if the lowest-energy state of the system is disorganized, and/or and kinetic origins, if the system experiences insurmountable barriers to achieving an organized state. Condensation of prepolymers with *N*,*N*-dimethylethylenediamine results in a similar loss of organization, supporting the hypothesis that the vinylogous urethane blocks have a lower χ parameter with PnBA compared to PAAEA. Nevertheless, a more polar diamine cross-linker also resulted in disorganized phase-separated morphologies, suggesting that kinetic barriers also play a role in hindering high-order organization of block copolymer-derived vitrimers that have been cross-linked in the disordered state. In order for hyperbranched polymers such as those shown in **Figure 8** to arrange themselves into a lamellar or cylindrical structure, the PnBA must be separated from the cross-linked PAAEA. Evolution of a regular periodic structure from a disorganized one requires the cooperative rearrangement of many domains at the same time, which would be impeded by the presence of the cross-links, even if they are dynamically active on the molecular level. We envision that such a reorganization would require

considerable energetically unfavorable molecular distortion to pack into a regular array that optimizes chain stretching and interfacial tension as required for a regular periodic morphology.

Permanently cross-linking a block copolymer in the disordered state, either in a melt above T_{ODT} or in a good solvent, can permit or prevent re-organization of the resulting network depending on cross-link density. Lightly cross-linked block copolymer networks re-assemble into organized morphologies upon cooling or solvent removal, but over a critical cross-link density, the networks are trapped in a disordered or disordered-like state.[73–76] Dynamic cross-links can also interfere with long-range order; there are several studies in which phase-separating block copolymers were cross-linked by H-bonds,[4,5] hindered urea dynamic covalent bonds,[77] or metal-ligand complexation.[6,7,78–80] In these examples, the cross-linked networks generally exhibit a single broad SAXS peak, consistent with disorganized phase-separated morphologies; corresponding transmission electron micrographs (TEMs), when available, reveal micellar or bicontinuous morphologies.[6,7,77] Interestingly, Noro and Matsushita could regain long-range order in their H-bonded block copolymer networks by adding a salt that interacted selectively with one block, raising the effective interaction parameter.[5] However, the kinetic barriers to reorganizing the H-bonded network are significantly lower than the barriers to reconfiguration in a vitrimer.

Most relevant to the present study, Epps and Sumerlin studied the assembly of methacrylic diblock copolymer vitrimers formed from bulk solution cross-linking and from solvent vapor annealing of self-assembled thin films with the cross-linker. While the thin films maintained the lamellar morphology after cross-linking, as shown by AFM and SAXS, the vitrimers formed from bulk cross-linking exhibited a single broad SAXS peak.[41] Presumably, cross-linking pre-assembled block copolymers in the solid state circumvents the kinetic barriers associated with reorganizing the network; however, transport limitations may restrict this strategy to thin films.

Based on our data and examples in the literature, we conclude that there are several challenges to achieving organized morphologies in pre-cross-linked block copolymer-derived vitrimers. Consideration must be given to the thermodynamics of mixing the blocks once the cross-linker is incorporated, particularly when the volume fraction of the cross-linked block is significant. In some CANs formed from homopolymer or small-molecule precursors, incorporation of the dynamic cross-links promotes phase separation.[70,81–83] The extent of cross-linking may also affect the barriers to reconfiguration, with lightly cross-linked networks more readily organized than highly cross-linked ones.[73] It remains to be determined whether the mechanism of dynamic covalent exchange, associative vs. dissociative, affects a network's ability to achieve organized morphologies. While increasing the χ parameter of the blocks, for example by replacing the PnBA block with polystyrene, will improve the driving force for phase separation, it will further increase the barriers to organization. For applications that require mechanically robust materials with transport through a continuous phase, such as filtration membranes[Error! Bookmark not defined.] and solid-state polymer electrolyte membranes,[84] the disorganized morphology of solution-annealed block copolymer vitrimers may in fact be advantageous.

Stress relaxation: relaxation times and activation energies do not increase with cross-linking. In the majority of reported vitrimers, increasing the cross-link density increases the relaxation time τ^* and the flow activation energy E_a.[29,85] These trends are convoluted by variations in the content of free nucleophile, which is why all our vitrimers were prepared with amounts of TREN that result in a constant 33 mol% excess free amine. Our lab has previously shown that changing the structure of the exchangeable group in the cross-linker can modulate stress relaxation rates through changes to τ_0 without affecting E_a.[27] In this work, vitrimers derived from block copolymers display a tunable modulus based on cross-link density over a wide range, but have nearly constant E_a. **Block-66-Net**, the most highly cross-linked material studied here, has slightly lower E_a (97 kJ/mol) compared to **Block-24-Net** through **Block-48-Net** (112–116 kJ/mol). The block copolymer vitrimers also have

nearly identical relaxation times at 160 ºC, with the exception of **Block-24-Net**, which has the lowest fraction of functional block but approximately 5 times slower stress relaxation. This work demonstrates that block copolymer composition offers a strategy to increase the stiffness of vitrimers without increasing reprocessing times.

To rationalize the observations in this paper, we turn to predictions by Ciarella and co-workers, based on molecular dynamics simulations of star polymer-based vitrimers. They hypothesized that loops would cause stress relaxation to be more facile.[86] Swapping an elastically-effective bond for another stress-bearing bond over short distances will not relax stress very much. On the other hand, swapping an elastically-effective bond for a loop removes the ability of that linkage to bear stress, causing relaxation. In complementary work, Ricarte and Shanbhag used an inhomogeneous Rouse model to show that vitrimers with blocky distributions of cross-linkers will relax stress faster than those with uniform cross-link distribution.[87] These theoretical studies, however, did not take microphase separation into account. Experimentally, like Epps and Sumerlin,[41] we do not observe that block copolymer vitrimers relax stress faster than compositionally similar statistical copolymers, and in fact retain a small amount of stress at long time scales (**Figure 5c**).

Stress relaxation rates in microphase-separated vitrimers represent a combination of the cross-link exchange rate, which is the rate-limiting step in homogeneous vitrimers above T_g, and the chain diffusion rate. Associative exchange events that occur within isolated cross-link-rich domains will not contribute significantly to stress relaxation. Ricarte and Leibler have proposed that in polyethylene/dioxaborolane vitrimers, the cross-linked segments of chains must disengage from cross-link-rich aggregates and diffuse through the cross-link-poor matrix to reduce topological stress, significantly hindering stress relaxation in self-assembled vitrimers compared to homogeneous

vitrimers.[88] These barriers to chain diffusion similarly explain the absence of terminal relaxation in block copolymer vitrimers.

In our microphase-separated system, diffusion on the length scales required to relax stress is expected to be faster through a continuous cross-link-rich phase compared to chain hopping between isolated cross-link-poor domains. Thus, increasing the volume fraction of cross-link-rich domains facilitates bond exchange across longer length scales, counterbalancing the effect of increasing cross-link density. The uniquely slow relaxation in **Block-24-Net** suggests that the cross-link-rich domains in this vitrimer are discontinuous (micellar or spherical-like, **Figure 11a**), while the other block copolymer vitrimers have continuous domains of the cross-link-rich phase (**Figure 11b**). Furthermore, following Ricarte and Leibler's logic, a strand bearing loops or dangling ends should disengage from the cross-link-rich domain and diffuse through the majority PnBA phase more readily than an elastically effective strand.[88] All the vitrimers contain some fraction of loops and dangling ends, but based on rubbery plateau moduli, we know that **Block-24-Net** has fewer network defects than **Block-34-Net**. We propose that the combination of lower volume fraction of the cross-linked block and fewer network defects dramatically hinders stress relaxation in **Block-24-Net**.

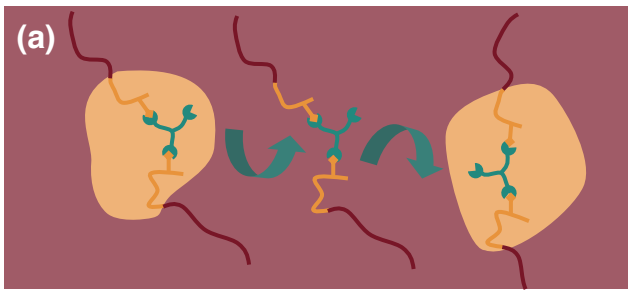

isolated cross-link-rich domains, fewer loops:
hinders chain diffusion

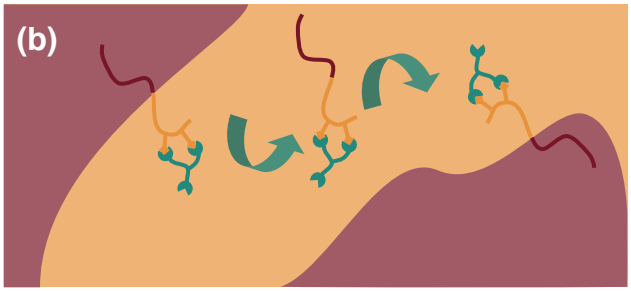

continuous cross-link-rich domains, more loops:
facilitates chain diffusion

Figure 11. Illustration of different factors that contribute to stress relaxation times in (a) **Block-24** and (b) **Block-34**. The yellow regions are the cross-linked PAAEA-rich phase, and the red matrix is the PnBA-rich phase. The green arrows indicate the path traversed by a strand to relax stress; for clarity, only selected strands are shown.

Conclusion

In this contribution, we explored the composition of block copolymer precursors as a design variable in vitrimers. Fundamentally, we show that the properties of this class of vitrimers are influenced by the interplay of microphase separation and network defects. The block sequence introduces more defects as a result of the adjacent cross-linking moieties, an effect further exacerbated by microphase separation in the dry state. Loops, in turn, shrink the domain size of the disorganized morphologies. We propose that rearrangement of these block copolymer vitrimers into organized morphologies is prevented by a combination of thermodynamic and kinetic factors. Microphase

separation also prevents direct comparison of these experimental results to theories describing the role of loops and block sequence on stress relaxation in vitrimers, which assume homogeneity.

Two experimental directions are recommended to provide clearer connections to theory. First, measurements of systems with decreased segregation strength, or of gels homogeneously swollen by a good solvent, are needed to precisely determine the effect of sequence on vitrimers in the absence of microphase separation. Secondly, quantification of the loop defects in vitrimers is required. Our lab is currently pursuing this latter goal using Network Disassembly Spectrometry.[89–91]

This study also presents several practical lessons for the design of vitrimers. First, block copolymers can be cross-linked in relatively concentrated (130–170 mg/mL) solutions to obtain soluble hyperbranched polymers. These solutions may be preferable for processing techniques that require lower viscosity. Upon solvent removal, vitrimers with high (≥94%) gel fraction are formed. Network defects must also be considered when targeting the appropriate functionality for prepolymers, as gel points significantly lower than calculated by Flory–Stockmayer or Carothers analysis are observed (**Block-13**). The moduli of the resulting materials will also reflect more network defects than in a homogeneous vitrimer, and may not increase monotonically by increasing prepolymer functionality. While these block copolymer vitrimers produced disorganized microphase-separated morphologies, we present considerations for future work seeking to achieve better organized morphologies. Block copolymers provide a convenient platform to increase the stiffness of vitrimers by increasing cross-link density, without affecting the flow activation energy or stress relaxation time. Finally, vinylogous urethane block copolymer vitrimers can be partially dissolved by heating in a good solvent. Further work is required to achieve complete solubilization of the vitrimer into hyperbranched polymers, which could present an alternative route to "chemical" recycling of hydrolytically stable vitrimers without any added nucleophilic reagents.

Supporting Information

Experimental procedures; sample preparation; NMR, FTIR, and UV-vis spectra; additional stress relaxation, DMTA, and SAXS data; details of cross-link density calculations

Corresponding Author

*jkalow@northwestern.edu

Acknowledgements

This work was supported by the NSF Center for Sustainable Polymers, CHE-1901635, and a seed grant from Northwestern's Center for Engineering Sustainability and Resilience. This work made use of the Integrated Molecular Structure Education and Research Center at Northwestern which has received support from the NIH (S10-OD021786-01); the NSF (NSF CHE- 9871268); Soft and Hybrid Nanotechnology Experimental (SHyNE) Resource (NSF ECCS-1542205); and the State of Illinois and International Institute for Nanotechnology. Rheological measurements were performed at the Materials Characterization and Imaging Facility which receives support from the MRSEC Program (NSF DMR-1720139) of the Materials Research Center at Northwestern University. Also used was the Keck-II facility of NU's NUANCE Center, which has received support from the SHyNE Resource, the MRSEC program at the Materials Research Center; the IIN, the Keck Foundation, and the State of Illinois, through the IIN. Parts of this work were carried out in the Characterization Facility, University of Minnesota, which receives partial support from NSF through the MRSEC program (DMR-2011401). This work used the 5-ID-D beamline of the DuPont-Northwestern-Dow Collaborative Access Team (DND-CAT) located at Sector 5 of the Advanced Photon Source (APS). DND-CAT is supported by E. I. DuPont de Nemours & Co., and The Dow Chemical Company, and State of Illinois funding to Northwestern University. This research used resources of the APS, a U.S.

Department of Energy (DOE) Office of Science User Facility operated for the DOE Office of Science by Argonne National Laboratory under Contract No. DE-AC02-06CH11357.

References

1. Bates, C. M.; Bates, F. S. 50th Anniversary Perspective: Block Polymers-Pure Potential. *Macromolecules* **2017**, *50*, 3–22.
2. Legge, N. R.; Holden, G.; Schroeder, H. E. *Thermoplastic Elastomers: A Comprehensive Review*; Hanser Publishers: Munich, 1987; Vol. 14.
3. Knoll, K.; Nießner, N. Styrolux+ and Styroflex+- From Transparent High Impact Polystyrene to New Thermoplastic Elastomers: Syntheses, Applications and Blends with Other Styrene Based Polymers. *Macromol. Symp.* **1998**, *132*, 231–243.
4. Chen, Y.; Kushner, A. M.; Williams, G. A.; Guan, Z. Multiphase Design of Autonomic Self-Healing Thermoplastic Elastomers. *Nat. Chem.* **2012**, *4*, 467–472.
5. Hayashi, M.; Matsushima, S.; Noro, A.; Matsushita, Y. Mechanical Property Enhancement of ABA Block Copolymer-Based Elastomers by Incorporating Transient Cross-Links into Soft Middle Block. *Macromolecules* **2015**, *48*, 421–431.
6. Mozhdehi, D.; Ayala, S.; Cromwell, O. R.; Guan, Z. Self-Healing Multiphase Polymers via Dynamic Metal-Ligand Interactions. *J. Am. Chem. Soc.* **2014**, *136*, 16128–16131.
7. Wang, W.; Zhang, J.; Jiang, F.; Wang, X.; Wang, Z. Reprocessable Supramolecular Thermoplastic BAB-Type Triblock Copolymer Elastomers with Enhanced Tensile Strength and Toughness via Metal–Ligand Coordination. *ACS Appl. Polym. Mater.* **2019**, *1*, 571–583.
8. Li, C. H.; Wang, C.; Keplinger, C.; Zuo, J. L.; Jin, L.; Sun, Y.; Zheng, P.; Cao, Y.; Lissel, F.; Linder, C.; You, X. Z.; Bao, Z. A Highly Stretchable Autonomous Self-Healing Elastomer. *Nat. Chem.* **2016**, *8*, 618–624.
9. Burattini, S.; Greenland, B. W.; Merino, D. H.; Weng, W.; Seppala, J.; Colquhoun, H. M.; Hayes, W.; MacKay, M. E.; Hamley, I. W.; Rowan, S. J. A Healable Supramolecular Polymer Blend Based on Aromatic π-π Stacking and Hydrogen-Bonding Interactions. *J. Am. Chem. Soc.* **2010**, *132*, 12051–12058.
10. Voorhaar, L.; Diaz, M. M.; Leroux, F.; Rogers, S.; Abakumov, A. M.; Van Tendeloo, G.; Van Assche, G.; Van Mele, B.; Hoogenboom, R. Supramolecular Thermoplastics and Thermoplastic Elastomer Materials with Self-Healing Ability Based on Oligomeric Charged Triblock Copolymers. *NPG Asia Mater.* **2017**, *9*, e385.
11. Wang, X.; Vapaavuori, J.; Zhao, Y.; Bazuin, C. G. A Supramolecular Approach to Photoresponsive Thermo/Solvoplastic Block Copolymer Elastomers. *Macromolecules* **2014**, *47*, 7099–7108.
12. Kloxin, C. J.; Bowman, C. N. Covalent Adaptable Networks: Smart, Reconfigurable and Responsive Network Systems. *Chem. Soc. Rev.* **2013**, *42*, 7161–7173.
13. Chakma, P.; Konkolewicz, D. Dynamic Covalent Bonds in Polymeric Materials. *Angew. Chemie - Int. Ed.* **2019**, *58*, 9682–9695.
14. Scheutz, G. M.; Lessard, J. J.; Sims, M. B.; Sumerlin, B. S. Adaptable Crosslinks in Polymeric Materials: Resolving the Intersection of Thermoplastics and Thermosets. *J. Am. Chem. Soc.* **2019**, *141*, 16181–16196.
15. Elling, B. R.; Dichtel, W. R. Reprocessable Cross-Linked Polymer Networks : Are Associative Exchange Mechanisms Desirable? *ACS Cent. Sci.* **2020**, *6*, 1488–1496.

16. Guerre, M.; Taplan, C.; Winne, J. M.; Du Prez, F. E. Vitrimers : Directing Chemical Reactivity to Control Material Properties. *Chem. Sci.* **2020**, *11*, 4855–4870.
17. Jourdain, A.; Asbai, R.; Anaya, O.; Chehimi, M. M.; Drockenmuller, E.; Montarnal, D. Rheological Properties of Covalent Adaptable Networks with 1,2,3-Triazolium Cross-Links: The Missing Link between Vitrimers and Dissociative Networks. *Macromolecules* **2020**, *53*, 1884–1900.
18. Jin, Y.; Lei, Z.; Taynton, P.; Huang, S.; Zhang, W. Malleable and Recyclable Thermosets : The Next Generation of Plastics. *Matter* **2019**, *1*, 1456–1493.
19. Scott, T. F.; Schneider, A. D.; Cook, W. D.; Bowman, C. N. Chemistry: Photoinduced Plasticity in Cross-Linked Polymers. *Science* **2005**, *308*, 1615–1617.
20. Montarnal, D.; Capelot, M.; Tournilhac, F.; Leibler, L. Silica-like Malleable Materials from Permanent Organic Networks. *Science* **2011**, *334*, 965–968.
21. Fortman, D. J.; Brutman, J. P.; Cramer, C. J.; Hillmyer, M. A.; Dichtel, W. R. Mechanically Activated, Catalyst-Free Polyhydroxyurethane Vitrimers. *J. Am. Chem. Soc.* **2015**, *137*, 14019–14022.
22. Self, J. L.; Dolinski, N. D.; Zayas, M. S.; Read De Alaniz, J.; Bates, C. M. Brønsted-Acid-Catalyzed Exchange in Polyester Dynamic Covalent Networks. *ACS Macro Lett.* **2018**, *7*, 817–821.
23. Nishimura, Y.; Chung, J.; Muradyan, H.; Guan, Z. Silyl Ether as a Robust and Thermally Stable Dynamic Covalent Motif for Malleable Polymer Design. *J. Am. Chem. Soc.* **2017**, *139*, 14881–14884.
24. Lu, Y. X.; Guan, Z. Olefin Metathesis for Effective Polymer Healing via Dynamic Exchange of Strong Carbon-Carbon Double Bonds. *J. Am. Chem. Soc.* **2012**, *134*, 14226–14231.
25. Liu, H.; Nelson, A. Z.; Ren, Y.; Yang, K.; Ewoldt, R. H.; Moore, J. S. Dynamic Remodeling of Covalent Networks via Ring-Opening Metathesis Polymerization. *ACS Macro Lett.* **2018**, *7*, 933–937.
26. Röttger, M.; Domenech, T.; Van Der Weegen, R.; Breuillac, A.; Nicolaÿ, R.; Leibler, L. High-Performance Vitrimers from Commodity Thermoplastics through Dioxaborolane Metathesis. *Science* **2017**, *356*, 62–65.
27. El-Zaatari, B. M.; Ishibashi, J. S. A.; Kalow, J. A. Cross-Linker Control of Vitrimer Flow. *Polym. Chem.* **2020**, *11*, 5339–5345.
28. Hayashi, M.; Yano, R. Fair Investigation of Cross-Link Density Effects on the Bond-Exchange Properties for Trans-Esterification-Based Vitrimers with Identical Concentrations of Reactive Groups. *Macromolecules* **2020**, *53*, 182–189.
29. Hajj, R.; Duval, A.; Dhers, S.; Avérous, L. Network Design to Control Polyimine Vitrimer Properties: Physical Versus Chemical Approach. *Macromolecules* **2020**, *53*, 3796–3805.
30. He, C.; Christensen, P. R.; Seguin, T. J.; Dailing, E. A.; Wood, B. M.; Walde, R. K.; Persson, K. A.; Russell, T. P.; Helms, B. A. Conformational Entropy as a Means to Control the Behavior of Poly(Diketoenamine) Vitrimers In and Out of Equilibrium. *Angew. Chemie - Int. Ed.* **2020**, *59*, 735–739.
31. Chen, X.; Li, L.; Wei, T.; Torkelson, J. M. Reprocessable Polymer Networks Designed with Hydroxyurethane Dynamic Cross-Links: Effect of Backbone Structure on Network Morphology, Phase Segregation, and Property Recovery. *Macromol. Chem. Phys.* **2019**, *220*, 1900083.
32. Ishibashi, J. S. A.; Kalow, J. A. Vitrimeric Silicone Elastomers Enabled by Dynamic Meldrum's Acid-Derived Cross-Links. *ACS Macro Lett.* **2018**, *7*, 482–486.
33. Guerre, M.; Taplan, C.; Nicolaÿ, R.; Winne, J. M.; Du Prez, F. E. Fluorinated Vitrimer

Elastomers with a Dual Temperature Response. *J. Am. Chem. Soc.* **2018**, *140*, 13272–13284.
34. Stukenbroeker, T.; Wang, W.; Winne, J. M.; Du Prez, F. E.; Nicolaÿ, R.; Leibler, L. Polydimethylsiloxane Quenchable Vitrimers. *Polym. Chem.* **2017**, *8*, 6590–6593.
35. Li, Y.; Liu, T.; Zhang, S.; Shao, L.; Fei, M.; Yu, H.; Zhang, J. Catalyst-Free Vitrimer Elastomers Based on a Dimer Acid: Robust Mechanical Performance, Adaptability and Hydrothermal Recyclability. *Green Chem.* **2020**, *22*, 870–881.
36. Wang, J.; Chen, S.; Lin, T.; Ke, J.; Chen, T.; Wu, X.; Lin, C. A Catalyst-Free and Recycle-Reinforcing Elastomer Vitrimer with Exchangeable Links. *RSC Adv.* **2020**, *10*, 39271–39276.
37. Yang, F.; Pan, L.; Ma, Z.; Lou, Y.; Li, Y.; Li, Y. Highly Elastic, Strong, and Reprocessable Cross-Linked Polyolefin Elastomers Enabled by Boronic Ester Bonds. *Polym. Chem.* **2020**, *11*, 3285–3295.
38. Liu, Z.; Zhang, C.; Shi, Z.; Yin, J.; Tian, M. Tailoring Vinylogous Urethane Chemistry for the Cross-Linked Polybutadiene: Wide Freedom Design, Multiple Recycling Methods, Good Shape Memory Behavior. *Polymer* **2018**, *148*, 202–210.
39. Spiesschaert, Y.; Taplan, C.; Stricker, L.; Guerre, M.; Winne, J. M.; Du Prez, F. E. Influence of the Polymer Matrix on the Viscoelastic Behaviour of Vitrimers. *Polym. Chem.* **2020**, *11*, 5377–5385.
40. Ishibashi, J. S. A.; Fang, Y.; Kalow, J. A. Exploiting Block Copolymer Phase Segregation to Tune Vitrimer Properties. 2019, ChemRxiv.org DOI: 10.26434/chemrxiv.10000232.v3.
41. Lessard, J. J.; Scheutz, G. M.; Sung, S. H.; Lantz, K. A.; Epps, T. H.; Sumerlin, B. S. Block Copolymer Vitrimers. *J. Am. Chem. Soc.* **2020**, *142*, 283–289.
42. Denissen, W.; Rivero, G.; Nicolaÿ, R.; Leibler, L.; Winne, J. M.; Du Prez, F. E. Vinylogous Urethane Vitrimers. *Adv. Funct. Mater.* **2015**, *25*, 2451–2457.
43. Denissen, W.; Droesbeke, M.; Nicolaÿ, R.; Leibler, L.; Winne, J. M.; Du Prez, F. E. Chemical Control of the Viscoelastic Properties of Vinylogous Urethane Vitrimers. *Nat. Commun.* **2017**, *8*, 14857.
44. Christopherson, C. J.; Hackett, Z. S.; Sauvé, E. R.; Paisley, N. R.; Tonge, C. M.; Mayder, D. M.; Hudson, Z. M. Synthesis of Phosphorescent Iridium-Containing Acrylic Monomers and Their Room-Temperature Polymerization by Cu(0)-RDRP. *J. Polym. Sci. Part A Polym. Chem.* **2018**, *56*, 2539–2546.
45. Lessard, J. J.; Garcia, L. F.; Easterling, C. P.; Sims, M. B.; Bentz, K. C.; Arencibia, S.; Savin, D. A.; Sumerlin, B. S. Catalyst-Free Vitrimers from Vinyl Polymers. *Macromolecules* **2019**, *52*, 2105–2111.
46. Chong, Y. K.; Moad, G.; Rizzardo, E.; Thang, S. H. Thiocarbonylthio End Group Removal from RAFT-Synthesized Polymers by Radical-Induced Reduction. *Macromolecules* **2007**, *40*, 4446–4455.
47. Carmean, R. N.; Figg, C. A.; Scheutz, G. M.; Kubo, T.; Sumerlin, B. S. Catalyst-Free Photoinduced End-Group Removal of Thiocarbonylthio Functionality. *ACS Macro Lett.* **2017**, *6*, 185–189.
48. Yamazaki, H.; Takeda, M.; Kohno, Y.; Ando, H.; Urayama, K.; Takigawa, T. Dynamic Viscoelasticity of Poly(Butyl Acrylate) Elastomers Containing Dangling Chains with Controlled Lengths. *Macromolecules* **2011**, *44*, 8829–8834.
49. Rudolph, T.; Schacher, F. H. Selective Crosslinking or Addressing of Individual Domains within Block Copolymer Nanostructures. *Eur. Polym. J.* **2016**, *80*, 317–331.
50. Strübe, F.; Rath, S.; Mattay, J. Functionalized Fulgides and Fluorophore-Photoswitch Conjugates. *European J. Org. Chem.* **2011**, *2011*, 4645–4653.
51. Snyder, R. L.; Lidston, C. A. L.; De Hoe, G. X.; Parvulescu, M. J. S.; Hillmyer, M. A.; Coates, G. W. Mechanically Robust and Reprocessable Imine Exchange Networks from Modular

Polyester Pre-Polymers. *Polym. Chem.* **2020**, *11*, 5346–5355.
52. Li, L.; Chen, X.; Jin, K.; Torkelson, J. M. Vitrimers Designed Both to Strongly Suppress Creep and to Recover Original Cross-Link Density after Reprocessing: Quantitative Theory and Experiments. *Macromolecules* **2018**, *51*, 5537–5546.
53. Easterling, C. P.; Kubo, T.; Orr, Z. M.; Fanucci, G. E.; Sumerlin, B. S. Chemical Science. *Chem. Sci.* **2017**, *8*, 7705–7709.
54. Lynd, N. A.; Hillmyer, M. A. Effects of Polydispersity on the Order-Disorder Transition in Block Copolymer Melts. *Macromolecules* **2007**, *40*, 8050–8055.
55. Sun, H.; Kabb, C. P.; Sims, M. B.; Sumerlin, B. S. Architecture-Transformable Polymers: Reshaping the Future of Stimuli-Responsive Polymers. *Prog. Polym. Sci.* **2019**, *89*, 61–75.
56. Breuillac, A.; Kassalias, A.; Nicolaÿ, R. Polybutadiene Vitrimers Based on Dioxaborolane Chemistry and Dual Networks with Static and Dynamic Cross-Links. *Macromolecules* **2019**, *52*, 7102–7113.
57. Schoustra, S. K.; Dijksman, J. A.; Zuilhof, H.; Smulders, M. M. J. Molecular Control over Vitrimer-like Mechanics – Tuneable Dynamic Motifs Based on the Hammett Equation in Polyimine Materials. *Chem. Sci.* **2021**, *12*, 293–302.
58. Taplan, C.; Guerre, M.; Winne, J. M.; Du Prez, F. E. Fast Processing of Highly Crosslinked, Low-Viscosity Vitrimers. *Mater. Horizons* **2020**, *7*, 104–110.
59. Spiesschaert, Y.; Guerre, M.; Imbernon, L.; Winne, J. M.; Du Prez, F. Filler Reinforced Polydimethylsiloxane-Based Vitrimers. *Polymer* **2019**, *172*, 239–246.
60. Gu, Y.; Kawamoto, K.; Zhong, M.; Chen, M.; Hore, M. J. A.; Jordan, A. M.; Korley, L. S. T. J.; Olsen, B. D.; Johnson, J. A. Semibatch Monomer Addition as a General Method to Tune and Enhance the Mechanics of Polymer Networks via Loop-Defect Control. *Proc. Natl. Acad. Sci. U. S. A.* **2017**, *114*, 4875–4880.
61. Sun, X.; Chwatko, M.; Lee, D. H.; Bachman, J. L.; Reuther, J. F.; Lynd, N. A.; Anslyn, E. V. Chemically Triggered Synthesis, Remodeling, and Degradation of Soft Materials. *J. Am. Chem. Soc.* **2020**, *142*, 3913–3922.
62. Nielsen, L. E. Cross-Linking–Effect on Physical Properties of Polymers. *J. Macromol. Sci. Part C* **1969**, *3*, 69–103.
63. Stutz, H.; Illers, K. -H; Mertes, J. A Generalized Theory for the Glass Transition Temperature of Crosslinked and Uncrosslinked Polymers. *J. Polym. Sci. Part B Polym. Phys.* **1990**, *28*, 1483–1498.
64. Fox, T. G.; Loshaek, S. Influence of Molecular Weight and Degree of Crosslinking on the Specific Volume and Glass Temperature of Polymers. *J. Polym. Sci.* **1955**, *15*, 371–390.
65. Sakurai, S.; Aida, S.; Nomura, S. Mechanical Properties of Polystyrene-Block-Polybutadiene-Block- Polystyrene Triblock Copolymers Crosslinked in the Disordered State. *Polymer* **1999**, *40*, 2071–2076.
66. Patel, S. K.; Malone, S.; Cohen, C.; Gillmor, J. R.; Colby, R. H. Elastic Modulus and Equilibrium Swelling of Poly(Dimethylsiloxane) Networks. *Macromolecules* **1992**, *25*, 5241–5251.
67. Flory, P. J.; Rehner, J. Statistical Mechanics of Cross-Linked Polymer Networks I. Rubberlike Elasticity. *J. Chem. Phys.* **1943**, *11*, 512–520.
68. Widmaier, J. M.; Sperling, L. H.; Widmaier, J. M. Phase Continuity in Sequential Poly(n-Butyl Acrylate)/Polystyrene Interpenetrating Polymer Networks. *Macromolecules* **1982**, *15*, 625–631.
69. Liu, Y.; Tang, Z.; Chen, J.; Xiong, J.; Wang, D.; Wang, S.; Wu, S.; Guo, B. Tuning the Mechanical and Dynamic Properties of Imine Bond Crosslinked Elastomeric Vitrimers by Manipulating the Crosslinking Degree. *Polym. Chem.* **2020**, *11*, 1348–1355.

70. Ricarte, R. G.; Tournilhac, F.; Leibler, L. Phase Separation and Self-Assembly in Vitrimers: Hierarchical Morphology of Molten and Semicrystalline Polyethylene/Dioxaborolane Maleimide Systems. *Macromolecules* **2019**, *52*, 432–443.
71. Hoff, E. A.; De Hoe, G. X.; Mulvaney, C. M.; Hillmyer, M. A.; Alabi, C. A. Thiol-Ene Networks from Sequence-Defined Polyurethane Macromers. *J. Am. Chem. Soc.* **2020**, *142*, 6729–6736.
72. Watanabe, K.; Katsuhara, S.; Mamiya, H.; Yamamoto, T.; Tajima, K.; Isono, T.; Satoh, T. Downsizing Feature of Microphase-Separated Structures via Intramolecular Crosslinking of Block Copolymers. *Chem. Sci.* **2019**, *10*, 3330–3339.
73. Sakurai, S.; Iwane, K.; Nomura, S. Morphology of Poly(Styrene-Block-Butadiene-Block-Styrene) Triblock Copolymers Cross-Linked in the Disordered State. *Macromolecules* **1993**, *26*, 5479–5486.
74. Vidil, T.; Hampu, N.; Hillmyer, M. A. Nanoporous Thermosets with Percolating Pores from Block Polymers Chemically Fixed above the Order-Disorder Transition. *ACS Cent. Sci.* **2017**, *3*, 1114–1120.
75. Hampu, N.; Hillmyer, M. A. Nanostructural Rearrangement of Lamellar Block Polymers Cured in the Vicinity of the Order-Disorder Transition. *Macromolecules* **2020**, *53*, 7691–7704.
76. Hahn, H.; Eitouni, H. B.; Balsara, N. P.; Pople, J. A. Responsive Solids from Cross-Linked Block Copolymers. *Phys. Rev. Lett.* **2003**, *90*, 155505.
77. Lee, H. M.; Perumal, S.; Kim, G. Y.; Kim, J. C.; Kim, Y. R.; Kim, M. P.; Ko, H.; Rho, Y.; Cheong, I. W. Enhanced Thermomechanical Property of a Self-Healing Polymer: Via Self-Assembly of a Reversibly Cross-Linkable Block Copolymer. *Polym. Chem.* **2020**, *11*, 3701–3708.
78. Zhang, J.; Li, M.; Cheng, L.; Li, T. Self-Healable and Tough Thermoplastic Materials from Metal–Thioether Block Polymers. *Macromol. Chem. Phys.* **2018**, *219*, 1700430.
79. Enke, M.; Bose, R. K.; Zechel, S.; Vitz, J.; Deubler, R.; Garcia, S. J.; Van Der Zwaag, S.; Schacher, F. H.; Hager, M. D.; Schubert, U. S. A Translation of the Structure of Mussel Byssal Threads into Synthetic Materials by the Utilization of Histidine-Rich Block Copolymers. *Polym. Chem.* **2018**, *9*, 3543–3551.
80. Bose, R. K.; Enke, M.; Grande, A. M.; Zechel, S.; Schacher, F. H.; Hager, M. D.; Garcia, S. J.; Schubert, U. S.; van der Zwaag, S. Contributions of Hard and Soft Blocks in the Self-Healing of Metal-Ligand-Containing Block Copolymers. *Eur. Polym. J.* **2017**, *93*, 417–427.
81. Chen, X.; Li, L.; Torkelson, J. M. Recyclable Polymer Networks Containing Hydroxyurethane Dynamic Cross-Links: Tuning Morphology, Cross-Link Density, and Associated Properties with Chain Extenders. *Polymer* **2019**, *178*, 121604.
82. Hayashi, M.; Chen, L. Functionalization of Triblock Copolymer Elastomers by Cross-Linking the End Blocks: Via Trans-N -Alkylation-Based Exchangeable Bonds. *Polym. Chem.* **2020**, *11*, 1713–1719.
83. Herbert, K. M.; Getty, P. T.; Dolinski, N. D.; Hertzog, J. E.; de Jong, D.; Lettow, J. H.; Romulus, J.; Onorato, J. W.; Foster, E. M.; Rowan, S. J. Dynamic Reaction-Induced Phase Separation in Tunable, Adaptive Covalent Networks. *Chem. Sci.* **2020**, *11*, 5028–5036.
84. Schulze, M. W.; McIntosh, L. D.; Hillmyer, M. A.; Lodge, T. P. High-Modulus, High-Conductivity Nanostructured Polymer Electrolyte Membranes via Polymerization-Induced Phase Separation. *Nano Lett.* **2014**, *14*, 122–126.
85. Soman, B.; Evans, C. M. Effect of Precise Linker Length, Bond Density, and Broad Temperature Window on the Rheological Properties of Ethylene Vitrimers. *Soft Matter* [Online early access]. DOI: 10.1039/D0SM01544J. Published Online: Nov 24, 2020.
86. Ciarella, S.; Sciortino, F.; Ellenbroek, W. G. Dynamics of Vitrimers: Defects as a Highway to

Stress Relaxation. *Phys. Rev. Lett.* **2018**, *121*, 58003.
87. Ricarte, R.; Shanbhag, S. Unentangled Vitrimer Melts: Interplay between Chain Relaxation and Cross-Link Exchange Controls Linear Rheology. *Macromolecules* [Online early access]. DOI: 10.1021/acs.macromol.0c02530. Published Online: Mar 17, 2021.
88. Ricarte, R. G.; Tournilhac, F.; Cloître, M.; Leibler, L. Linear Viscoelasticity and Flow of Self-Assembled Vitrimers: The Case of a Polyethylene/Dioxaborolane System. *Macromolecules* **2020**, *53*, 1852–1866.
89. Zhou, H.; Woo, J.; Cok, A. M.; Wang, M.; Olsen, B. D.; Johnson, J. A. Counting Primary Loops in Polymer Gels. *Proc. Natl. Acad. Sci. U. S. A.* **2012**, *109*, 19119–19124.
90. Zhong, M.; Wang, R.; Kawamoto, K.; Olsen, B. D.; Johnson, J. A. Quantifying the Impact of Molecular Defects on Polymer Network Elasticity. *Science* **2016**, *353*, 1264–1268.
91. Wang, J.; Wang, R.; Gu, Y.; Sourakov, A.; Olsen, B. D.; Johnson, J. A. Counting Loops in Sidechain-Crosslinked Polymers from Elastic Solids to Single-Chain Nanoparticles. *Chem. Sci.* **2019**, *10*, 5332–5337.